ECG Morphological Decomposition for Automatic Rhythm Identification

Guadalupe García-Isla[1], Rita Laureanti[1], Valentina D. Corino[1], Luca T. Mainardi[1]

[1]Department of Electronics, Information and Bioengineering, Politecnico di Milano, Milan, Italy

Abstract

Manual rhythm classification in 12-lead ECGs is time-consuming and operator-biased. We present an automatic ECG classifier using CinC's 2020 challenge dataset. In the first phase of the Challenge, 9 categories were targeted with an ensemble of 4 classifiers. In the second phase, 7 classifiers were implemented to detect 24 cardiac electrophysiological disorders. Five classifiers identified abnormalities in different specific regions of the heart's conducting system. Two classifiers were dedicated to detect premature atrial and ventricular contractions.

The methodology is based on the creation of rhythm-specific intra and inter-patient templates. Firstly, signals were divided into 6 regions of interests. Secondly, for each region, intra-patient models and inter-patient rhythm-specific models were computed. The distances from each intra-patient model to each rhythm-specific inter-patient model as well as heart rate variability features and Global Electric Heterogeneity features were introduced into the classifiers.

After a 10-fold cross-validation, for the provided training data in the first phase an accuracy of 94.4%±0.4, and a Challenge metric of 0.644±0.031 were obtained, whereas in the second phase an accuracy and Challenge metric of 15.0 ± 1.0 % and 0.030 ± 0.009 were obtained.

1. Introduction

Cardiovascular diseases (CVDs) are the first cause of mortality and morbidity worldwide [1]. The standard 12-lead electrocardiogram (ECG) is an essential tool in clinical practice to diagnose CVDs and to have an initial assessment of a patient's health condition [2]. Typically, manual interpretation of ECGs by expert clinicians is needed. This requires skilled personnel with high degree of specialization and in some cases inter-operators discrepancies are present. An automatic algorithm for detection of cardiac abnormalities and classification of ECG recordings could aid clinical practice, providing clinicians with an objective tool to make an early and accurate diagnosis of CVDs [3]. The aim of this work is to put together machine learning techniques and physiological know-how to build and validate such model, using the 6 annotated datasets available for the 2020 Computing in Cardiology Challenge [4] (team name: *Germinating)*.

2. Material and Methods

2.1. Data

Six databases were provided: China Physiological Signal Challenge in 2018 (CPSC2018), St Petersburg INCART 12-lead Arrhythmia Database, the PTB Diagnostic ECG Database, the PTB-XL electrocardiography Database and the Georgia 12-Lead ECG Challenge Database. In total, 43,101 labeled 12-lead ECGs with 111 different cardiac abnormalities labelled following the SNOMED-CT coding system. Only 24 disorders were targeted: 1st degree AV block (IAVB), atrial fibrillation (AF), atrial flutter (AFL), bradycardia (Brady), incomplete right bundle branch block (IRBBB), left anterior fascicular block (LAnFB), left axis deviation (LAD), left bundle branch block (LFBBB), low QRS voltages (LQRSV), nonspecific intraventricular conduction disorder (NSIVCB), pacing rhythm (PR), premature atrial complex (PAC), premature ventricular complex (PVC), prolonged PR interval (LPR), prolonged QT interval (LQT), Q-wave abnormal (QAb), right axis deviation (RAD), sinus arrhythmia (SA), sinus bradycardia (SB), normal sinus rhythm (NSR), sinus tachycardia (STach), T-wave abnormal (TAb) and T-wave inversion (TInv), the rest were considered "Unscored" and ignored. For the first phase, also ST elevation (STE) and depression (STD) were considered.

2.1. ECG preprocessing

Two median filters were applied to obtain the baseline of each ECG signal that was then subtracted to the original ECG to obtain a baseline corrected signal. Power line and high-frequency noise were removed with a finite impulse response low-pass filter with equal ripple in the pass and stop bands. The 3-dB point of the filter was 35 Hz. R peaks were detected using Pan Tompkins' algorithm [5]. To minimize misdetections, R peaks were detected on 5 leads with positive QRS (I, II, III, aVF, V4, V5, V6). An impulse

train signal was built based on the R peaks detected for each lead; a Gaussian filter was applied to smooth the R series, then signals were aligned through a cross-correlation procedure, using V5 as reference and finally the median signal among the 5 series was computed. On the obtained signal, the Pan Tomkins algorithm was applied to obtain the R peaks used on the rest of the analysis.

2.2. Heart rate variability features

The mean and standard deviation of the RR intervals was computed, along with the standard deviation of the difference of consecutive RR intervals, the percentage of successive interval differences greater than 50 ms (pNN50) and the root mean square of successive differences (RMMSD).

2.3. Intra and inter-patient models

Inter-patient models that gathered the median behaviour of each electrohpysiological disorder in the ECG were built for different signal segments of clinical significance. These models were used to measure the distance of each patient to the ECG pattern typical of each electrophysiological disorder.

Firstly, ECG windows of interest were selected based on the expected occurrence of different electrical events (all values referred to the location of R peak): P-wave (from -300 ms to -40 ms) [6], QRS-complex (-70 ms to +60 ms), PQ-ST (PT-segment with the removal of the QRS-segment, from -150 ms to +250 ms, removing the segment from -55 ms to + 55 ms), T-wave (from +100 ms to +350 ms) [7], PR (from -288 ms to the R peak), RT (from the R peak to +258 ms).

Secondly, intra-patient templates were computed for each of the above-mentioned segments. For each lead, all windows were aligned and the median waveform, representative of the analyzed subject, was calculated. The mean standard deviation of all windows was stored as a feature. Thirdly, the maximum cross-correlation index was computed between each individual region of interest and the median intra-patient template. Fourthly, for each rhythm, the templates of the correspondent subjects of the training set were aligned and the median rhythm template was obtained. Finally, the maximum cross-correlation between each intra-patient templates and each of the inter-patient models with the corresponding lags were stored as features. In Figure 1, an example is visible for the RT segment for NSR, RBBB and LBBB. On the left panels, all RT segments in the recording of a subject are depicted with the obtained intra-patient template in red. On the right, the median intra-patient templates of all the subjects are plotted with the resulting inter-patient template in red.

2.4. GEH features

Global Electric Heterogeneity (GEH) features were computed using the three open source toolboxes provided by the challenge: HRV toolbox [8], ECGkit [9] and GEH parameter extraction [10], [11] and origin point [12]. These features included: azimuth, elevation, and magnitude of spatial peak QRS, T and spatial ventricular gradient (SVG) vectors, azimuth and elevation of QRS, T vectors and Wilson's area SVG, scalar value of the SVG, and peak and are of the spatial QRS-T angle [10], [11].

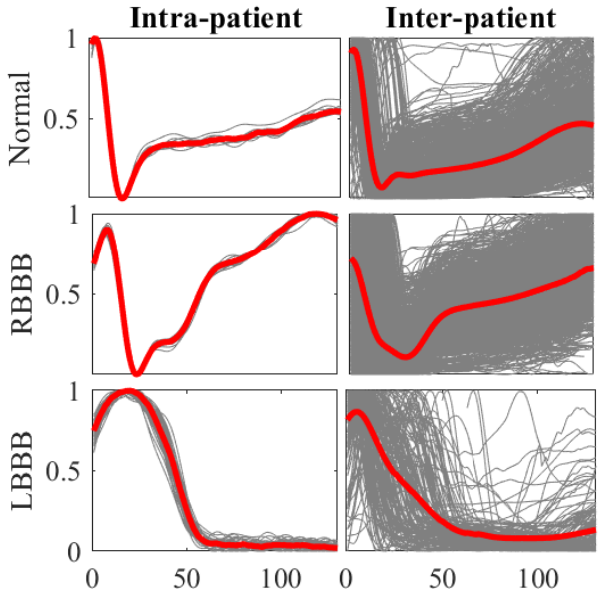

Figure 1. Intra and inter-patient templates for the RT segment of the rhythms Normal, RBBB and LBBB. All the segments of a recording are overlapped in the intra-patient plots, whereas in the inter-patients plots, the median segments of all the subjects with the respective condition are depicted. The median segments are in red.

2.5. Classifier ensemble

The classification strategy adopted was to create an ensemble of classifiers, each of them focused on a specific region of the cardiac conductive system. A distinction was made between sporadic conditions as PAC and PVC, and stable conditions, all the other pathologies. As most signals ranged from 6 s to 60 s, all arrhythmias were considered present on the whole signal.

During phase 1, the detection of permanent conditions was distributed into different classifiers depending on the ECG region where the electrophysiological disorders were manifested (Table 1). This yielded one classifier (C1) including the cross-correlation values between inter-patient and intra-patient of the P-wave and PR interval, and another one (C2) including the QRS complex, RT segment and T-wave information. Both classifiers included GEH and HRV features, as well as age and sex.

Given the increase in the amount of rhythms included in phase 2, the detection of permanent conditions was

distributed differently, according to the cardiac region of occurrence:

- C1: Atrial tissue
- Purkinje system
  - C2: Sinoatrial node
  - C3: Atrioventricular (AV) node
  - C4: Bundle branches
- C5: Ventricular tissue

Cross-correlation values between inter-patient and intra-patient models were included as: P-wave and PR segments for C1 and C3, all segments for C2, and QRS complex, PQ-ST segment, T wave, and RT segment for C4 and C5. HRV and GEH features as well as age and sex were included in all classifiers.

For each of the sporadic conditions (PAC and PVC) an individual classifier was designed in both phases, which led to a total of 4 classifiers in phase 1 and 7 in phase 2. C6 and C7 included all the HRV features and the cross-correlation values between the intra-patient template and the 3 beats with the shortest preceding RR interval for the QSR and P-wave segments. Signals classified as AF or AFL were not taken into consideration for possible PAC or PVC.

In phase 1, C1 and C2 were support vector machines. PAC and PVC classifiers used bagged trees. For the second phase, in which 24 categories were included, all classifiers used boosted trees. All classifiers were implemented in Matlab 2020a and trained using a 10-fold cross-validation.

3. Results

The results obtained after the 10-fold cross-validation of the provided datasets for phase 1 and 2 of the challenge are gathered in Tables 1 and 2, respectively. Sensitivity and specificity values are displayed along with the number of signals present in the dataset for each rhythm of study. In addition, the sub-indexes C1, C2, …, C7 in the Rhythms column indicate the classifier in which the rhythm was included. In both phases specificity (Sp.) values were higher than sensitivity (Se.) ones. Results in phase 1 were superior than those in phase 2. Categories not detected by the classifier in phase 2 have been excluded from Table 2.

Table 3 gathers the overall results obtained for the classifier ensembles of phases 1 and 2 after a 10-fold cross-validation on the databases provided. The Challenge Metric (CM) used to evaluate the classifiers varied from phase 1 to phase 2. While in phase 1 it corresponded to the geometrical mean between F_β measure and G_β measure, on phase 2 a new scoring system was used to reflect the value of the algorithm in a clinical setting: it awarded full credit to correct diagnoses and partial credit to misdiagnoses with similar risks or outcomes similar to those of the actual diagnosis.

Table 1. Classification results on the test set after 10-fold cross-validation on the CPSC dataset labelled according to the first phase of the challenge.

Rhythms	Subjects	Se(%)	Sp(%)
AF_{C1}	1221	94.6±0.02	95.9±0.01
$IAVB_{C1}$	722	88.1±0.05	97.1±0.01
$LBBB_{C2}$	236	85.6±0.08	98.5±0.00
NSR	918	78.8±0.04	93.7±0.01
PAC_{C3}	616	84.5±0.06	90.3±0.01
PVC_{C4}	700	87.8±0.02	93.5±0.01
$RBBB_{C2}$	1857	89.5±0.02	96.5±0.01
STD_{C2}	869	69.6±0.05	96.8±0.01
STE_{C2}	220	37.2±0.09	99.3±0.00

Table 2. Classification results on the test set after 10-fold cross-validation on all the datasets labelled according to the second phase of the challenge.

Rhythms	Subjects	Se(%)	Sp(%)
AF_{C1}	3475	94.55±1.19	93.97±0.56
AFL_{C1}	314	16.33±6.77	99.70±0.10
$IAVB_{C3}$	2394	92.32±1.82	81.08±1.76
$IRBBB_{C4}$	1611	5.78±2.43	99.77±0.14
LAD_{C4}	6086	56.52±5.13	86.84±0.83
$LAnFB_{C4}$	1806	56.29±14.67	97.60±0.58
$LBBB_{C4}$	1041	31.38±3.64	99.71±0.09
LQT_{C5}	1513	8.91±2.98	99.08±0.54
PAC_{C6}	1944	65.88±4.20	91.61±0.84
PVC_{C7}	1253	50.22±7.17	85.36±1.45
$RBBB_{C4}$	3085	89.53±2.39	95.70±0.52
SB_{C2}	2359	43.20±2.69	98.95±0.20
NSR_{C2}	20846	90.48±0.61	70.38±1.55
$STach_{C2}$	2402	86.78±2.91	99.25±0.20
TAb_{C5}	4673	56.57±7.34	78.75±4.07

Table 3. Classification results on phase 1 and 2 for 10-fold cross-validation of the provided datasets.

Ph.	AUROC	AUPRC	Accuracy	F	Fbeta	Gbeta	CM
1st	0.099±0.009	0.019±0.002	0.944±0.004	0.727±0.019	0.763±0.019	0.525±0.025	0.644±0.031
2nd	0.541±0.002	0.083±0.001	0.148±0.009	0.116±0.004	0.144±0.004	0.062±0.002	0.030±0.009

Ph=phase; AUROC=area under the receiver operating curve; AUPRC=area under the precision-recall curve.

4. Discussion

The aim of this work was to propose an automatic algorithm capable of identifying different cardiovascular diseases using 6 different databases with 43,101 labeled recordings made available by the PhysioNet/Computing in Cardiology Challenge 2020 [4]. Several attempts have been already described in literature [3], [13], [14], [15]. Currently, the role of clinicians is still fundamental for the final diagnosis, but a support role from computers could provide a useful tool to aid them for early and correct diagnosis of cardiac abnormalities.

The presented method intended to follow a physiologically consistent approach. An ensemble of classifiers was built focusing each of them on specific cardiac regions. The electrophysiological disorders of study were distributed into each of the classifiers depending or their region of incidence. ECG signals were divided into regions of interest and a comparison was performed between intra-patient models and inter-patient rhythm-specific models. In phase 1 the methodology succeeded in detecting all disorders with specificity higher than 90% and sensitivity higher than 84%, except for STE and STD. These results are in line with those already present in literature [15], although as different databases are used, a comparison is not trivial. These results suggest that intra-patient and inter-patient models manage to capture electrophysiological disturbances of different nature and areas of the cardiac tissue.

However, results obtained in phase 2 show that the metrics used are not enough if a larger number of conditions with often similar expression in the ECG are targeted, as IRBBB and RBBB, IAVB and LPR, LAnFB and LBBB, among others. In each classifier (C1, C2, …, C7) at least a cardiac abnormality was detected with good results i.e. AF in C1, STach in C2, IAVB in C3, RBBB in C4. However, the models built and/or the metric obtained seemed to be unable to distinguish among such an amount of rhythms exhibiting similar morphologies.

5. Conclusion

We obtained promising results for the detection of a limited number of electrophysiological abnormalities in short signals. Further development is needed for its application to a high number of disorders, possibly through the implementation of convolutional neural network.

Acknowledgments

This project is framed inside MY-ATRIA consortium. MY-ATRIA project has received funding from the European Union's Horizon 2020 research and innovation program under the Marie Skłodowska-Curie grant agreement No.766082.

References

[1] M. F. Piepoli *et al.*, "2016 European Guidelines on Cardiovascular Disease Prevention in Clinical Practice," *Eur. Heart J.*, vol. 37, no. 29, pp. 2315–2381, 2016.

[2] N. Peters, M. A. Gatzoulis, and R. Vecht, *ECG Diagnosis in Clinical Practice*, Second. Springer, 2009.

[3] H. Smulyan, "The Computerized ECG: Friend and Foe," *Am. J. Med.*, vol. 132, pp. 153–160, 2019.

[4] E. A. Perez Alday *et al.*, "Classification of 12-lead ECGs: the PhysioNet/Computing in Cardiology Challenge 2020," *Physiol. Meas.*, 2020.

[5] J. Pan and W. J. Tompkins, "A Real-Time QRS Detection Algorithm," *IEEE Trans. Biomed. Eng.*, vol. BME-32, no. 3, pp. 230–236, 1985.

[6] F. Censi *et al.*, "P-Wave Morphology Assessment by a Gaussian Functions-Based Model in Atrial Fibrillation Patients," *IEEE Trans. Biomed. Eng.*, vol. 54, no. 4, pp. 663–672, 2007.

[7] G. Goovaerts, C. Varon, B. Vandenberk, R. Willems, and S. Van Huffel, "Tensor-based Detection of T wave Alternans in Multilead ECG Signals," in *Computing in Cardiology*, 2014.

[8] A. N. Vest *et al.*, "An Open Source Benchmarked Toolbox for Cardiovascular Waveform and Interval Analysis," *Physiol. Meas.*, vol. 39, no. 10, p. 105004, 2018.

[9] A. J. Demski and M. Llamedo Soria, "ecg-kit a Matlab Toolbox for Cardiovascular Signal Processing," *J. Open Res. Softw.*, vol. 4, no. 1, p. e8, 2016.

[10] J. W. Waks *et al.*, "Global Electric Heterogeneity Risk Score for Prediction of Sudden Cardiac Death in the General Population: The Atherosclerosis Risk in Communities (ARIC) and Cardiovascular Health (CHS) Studies," *Circulation*, vol. 133, pp. 2222–2234, 2016.

[11] J. A. Thomas *et al.*, "Vectorcardiogram in Athletes: The Sun Valley Ski Study," *Ann. Noninvasive Electrocardiol.*, p. e12614, 2018.

[12] E. A. Perez-Alday *et al.*, "Importance of the Heart Vector Origin Point Definition for an ECG Analysis: The Atherosclerosis Risk in Communities (ARIC) Study," *Comput. Biol. Med.*, vol. 104, pp. 127–138, 2019.

[13] M. Alfaras, M. C. Soriano, and S. Ortín, "A Fast Machine Learning Model for ECG-based Heartbeat Classification and Arrhythmia Detection," *Front. Phys.*, vol. 7, p. 103, 2019.

[14] J. Schläpfer and H. J. Wellens, "Computer-Interpreted Electrocardiograms: Benefits and Limitations," *J. Am. Coll. Cardiol.*, vol. 70, no. 9, pp. 1183–1192, 2017.

[15] X. Zhang *et al.*, "Automated Detection of Cardiovascular Disease by Electrocardiogram Signal Analysis: A Deep Learning System," *Cardiovasc. Diagn. Ther.*, vol. 10, no. 2, pp. 227–235, 2020.

Address for correspondence:

Guadalupe García Isla
Via Camillo Golgi, 39, 20133 Milano, Italy
guadalupe.garcia@polimi.it